Original Article

Dlx5 and Mef2 Regulate a Novel Runx2 Enhancer for Osteoblast-Specific Expression†

Tetsuya Kawane[1§], Hisato Komori[1§], Wenguang Liu[1, 2], Takeshi Moriishi[1], Toshihiro Miyazaki[1], Masako Mori[1], Yuki Matsuo[1], Yoshio Takada[3], Shinichi Izumi[1], Qing Jiang[1], Riko Nishimura[4], Yosuke Kawai[1, 5], and Toshihisa Komori[1]*

[1]Department of Cell Biology, Unit of Basic Medical Sciences, [5]Department of Regenerative Oral Surgery, Unit of Translational Medicine, Nagasaki University Graduate School of Biomedical Sciences, Nagasaki, Japan: [2]Institute of Genetics & Cytology, Northeast Normal University, Changchun, China; [3]Laboratory for Pharmacology, Pharmaceuticals Research Center, Asahi Kasei Pharma Corporation, Shizuoka, Japan; [4]Department of Molecular and Cellular Biochemistry, Osaka University Graduate School of Dentistry, Osaka, Japan.

[§]Tetsuya Kawane and Hisato Komori contributed equally to this work

*Corresponding author: Department of Cell Biology, Unit of Basic Medical Sciences, Nagasaki University Graduate School of Biomedical Sciences, 1-7-1 Sakamoto, Nagasaki 852-8588, Japan
TEL: +81-95-819-7630; FAX: +81-95-819-7633; E-mail: komorit@nagasaki-u.ac.jp

Additional Supporting Information may be found in the online version of this article.

Initial Date Submitted November 28, 2013; Date Revision Submitted March 2, 2014; Date Final Disposition Set March 12, 2014

Journal of Bone and Mineral Research

DOI 10.1002/jbmr.2240

Abstract

Runx2 is essential for osteoblast differentiation and chondrocyte maturation. The expression of Runx2 is the first requisite step for the lineage determination from mesenchymal stem cells to osteoblasts. Although the transcript from *Runx2* distal promoter is majorly expressed in osteoblasts, the promoter failed to direct green fluorescent protein (GFP) expression to osteoblasts. To find the regulatory region, we generated GFP reporter mice driven by a bacterial artificial chromosome (BAC) of *Runx2* locus, and succeeded in the reproduction of endogenous *Runx2* expression. By serially deleting it, we identified a 343 bp enhancer, which directed GFP expression specifically to osteoblasts, about 30 kb upstream of the distal promoter. The sequence of the 343 bp enhancer was highly conserved among mouse, human, dog, horse, opossum, and chicken. Dlx5, Mef2c, Tcf7, Ctnnb1, Sp7, Smad1, and Sox6, which localized on the enhancer region in primary osteoblasts, synergistically upregulated the enhancer activity, whereas Msx2 downregulated the activity in mouse osteoblastic MC3T3-E1 cells. Msx2 was predominantly bound to the enhancer in mouse multipotent mesenchymal C3H10T1/2 cells, whereas Dlx5 was predominantly bound to the enhancer in MC3T3-E1 cells. Dlx5 and Mef2 directly bound to the enhancer and the binding sites were required for the osteoblast-specific expression in mice, while the other factors bound to the enhancer by protein-protein interaction. The enhancer was characterized by the presence of the histone variant H2A.Z, the enrichment of histone H3 mono- and dimethylated at Lys4 and acetylated at Lys18 and Lys27, but the depletion of histone H3 trimethylated at Lys4 in primary osteoblasts. These findings indicated that the enhancer, which had typical histone modifications for enhancers, contains sufficient elements to direct *Runx2* expression to osteoblasts, and that Dlx5 and Mef2, which formed an enhanceosome with Tcf7, Ctnnb1, Sp7, Smad1, and Sox6, play an essential role in the osteoblast-specific activation of the enhancer.

Key words: Runx2, Dlx5, Mef2, enhancer, osteoblast

Introduction

Runx2 is a transcription factor that regulates two lineages of mesenchymal cells, osteoblasts and chondrocytes, during skeletal development.[1] Runx2 is expressed as two isoforms (type I Runx2 starting with the sequence MRIPV and type II Runx2 starting with the sequence MASNS) that possess different N-termini and are expressed under the proximal (P2) and distal (P1) promoters, respectively.[2] Both type I and II *Runx2* isoforms are expressed in chondrocytes, as well as osteoblasts, but type II *Runx2* expression is predominant in osteoblasts and considered to be important for osteoblast differentiation.[3] Although transcriptional regulation of *Runx2* was investigated in the P1 promoter,[2, 4-8] reporter mice under the control of P1 promoter failed to express the reporter gene in osteoblasts.[9] *Runx2* expression in an osteoblastic lineage at appropriate times and sites is essential for bone development and maintenance.[10] Further, permanent cartilage enters the process of endochondral ossification in the presence of Runx2, and heterodeficiency of *Runx2* reduces the severity of osteoarthritis, indicating that Runx2 is involved in the deterioration of permanent cartilage.[11, 12] Therefore, it is important to discriminate the transcriptional regulation of *Runx2* gene in osteoblasts and chondrocytes for the regeneration of bone and cartilage. However, the transcriptional regulation of *Runx2* remains to be clarified.

We searched for regulatory elements of the *Runx2* gene, and identified a 343 bp enhancer sequence, which specifically directed the reporter gene expression to osteoblasts. We show here the molecular mechanism of *Runx2* expression in osteoblasts.

Materials and Methods

Plasmid Construction

The 343 bp enhancer fragment was subcloned into minimal promoter (mP)-pGL4.10, and deletion constructs of the 343 bp fragment were generated by PCR and subcloned into 343-mP-pGL4.10 or pBluescript II with Hsp68 minimal promoter and enhanced GFP (eGFP).

Generation of transgenic (tg) mice

To generate the reporter mice of a BAC clone, the 200 kb fragment of mouse *Runx2* region in a BAC clone (RP23-356F5, Source BioScience) was subcloned into IRES-eGFP-polyA-containing vector, and the inserted fragment was serially deleted using the counter-selection BAC modification kit (Gene Bridges). Prior to the study, all experiments were reviewed and approved by the Animal Care and Use Committee of Nagasaki University Graduate School of Biomedical Sciences.

Histological analysis

Embryos at E16.5 were fixed with 4% paraformaldehyde at 4°C for 2 hours, washed with PBS at 4°C for 1 hour, immersed in 20% sucrose at 4°C overnight, embedded in O. C. T. Compound (Sakura Finetek), and sectioned at 7μm thickness using Leica CM3050S (Leica Biosystems).

Luciferase assay, real-time RT-PCR analysis, and ChIP assay

Luciferase assay, real-time RT-PCR analysis, and ChIP assay were performed as described previously.[13] In luciferase assays, the data are presented as means±SEM (n=3). We normalized the values to that of *β-actin* in real-time RT-PCR analysis. Primer sequences and the information of the antibodies are shown in Supplemental

Table 1 and 2. A cDNA library was constructed and screening was performed using pGL4.23 (Promega) containing 4 x 343 bp in SaOS2 cells as previously described. [14]

Electrophoretic mobility shift assay (EMSA)

Proteins of transcription factors were generated by *in vitro* transcription/translation using the T7 Coupled TNT Rabbit Reticulocyte Lysate System (Promega), and EMSA was performed as previously described.[15] The information of the antibodies and the sequences of the oligonucleotides are shown in Supplemental Table 1 and 2.

Glutathione S-transferase (GST)-pulldown experiments

GST fusion proteins were expressed in BL21(DE3)pLysS (BioDynamics Laboratory) by using pGEX4T vectors and immobilized on glutathione sepharose 4B (GE Healthcare). Nuclear extracts or the cytosol fraction (for flag-EGFP) was incubated with immobilized GST fusion proteins. After extensive washes, bound proteins were eluted and analyzed by Western blotting using anti-flag antibody (M2 Sigma).

Results

Reporter gene expression under the control of P1 promoter of *Runx2*

To examine the genomic regions required for bone-specific expression of *Runx2*, we first generated GFP or lacZ tg mice under the control of 1.9 kb, 2.3 kb, 6.1 kb, or 7 kb P1 promoter of *Runx2* (Supplemental Fig. 1 and data not shown). Strong GFP expression was detected in the head of the tg mice using 6.1 kb P1 promoter (Supplemental Fig. 1B). GFP was strongly expressed in neurons in the brain and spinal cord, mesenchymal

cells around the tooth buds, and subcutaneous connective tissue in the head; very weakly detected in perichondrium of rib and immature chondrocytes in vertebrae; barely detectable in osteoblasts in calvaria, mandible and limb bones; and undetectable in chondrocytes of the growth plates in limb bones (Supplemental Fig. 1C-K).

Generation of reporter mice using a BAC clone of *Runx2* gene locus

To determine the *Runx2* gene locus, which covers the entire regulatory elements for *Runx2* expression, we generated GFP tg mice using a BAC clone of *Runx2* gene locus (Fig. 1A). The tg (200kR GFP tg) mice showed GFP expression in skeletons (Fig. 1B, C). GFP expression was detected in osteoblasts and chondrocytes in whole skeletons (Fig. 2C, D). Next, we serially deleted the 5' region from exon 1 and generated GFP tg (Δ1st GFP tg, Δ2nd GFP tg, and Δ3rd GFP tg) mice (Fig. 1A). Both the Δ2nd GFP tg mice and Δ3rd GFP tg mice showed a similar pattern of GFP expression as the 200kR GFP tg mice (Fig. 1B, C, F-I, 2C, D, G-J, Supplemental Fig. 2). In Δ1st GFP tg mice, however, GFP expression was barely detectable in the skeletons (Fig. 1D, E), and GFP was barely detectable in osteoblasts of mandible in Δ1st GFP tg mice (Supplemental Fig. 3). Although GFP expression was detected around eyeballs in all of the tg mice, it was derived from the frontal bones, zygomatic bones, and maxillas in 200kR, Δ2nd, and Δ3rd GFP tg mice, whereas it was derived from the connective tissue and the periosteum of zygomatic bones in Δ1st GFP tg mice (Fig. 1J-Q and data not shown). Further, GFP expression in osteoblasts in the frontal bones, maxillas, and inside of zygomatic bones was barely detectable in Δ1st GFP tg mice (Fig. 1J-M). The expression levels and frequencies of GFP-positive osteoblasts

were severely reduced, and expression in chondrocytes was also reduced (Fig. 2E, F, Supplemental Fig. 4). Although GFP-positive cells were detected in the perichondrium and bone collar in the femurs of Δ1st GFP tg mice, the intensities were severely reduced compared with those in Δ2nd and Δ3rd GFP tg mice, because the GFP signal was undetectable without a longer exposure (Fig. 2F, J, Supplemental Fig. 5). In contrast to the weak expression in skeletal cells, GFP was strongly detected in the connective tissue around the eyeballs and salivary glands (Supplemental Fig. 4).

Identification of 1.3 kb osteoblast-specific enhancer

As the P1 promoter was deleted in the Δ1st GFP construct, it may have caused the drastic reduction of GFP expression in osteoblasts and chondrocytes in Δ1st GFP tg mice. However, the 6.1 kb P1 promoter was not enough to direct reporter gene expression to osteoblasts (Supplemental Fig. 1). Thus, we speculated that a regulatory element might be present in the deleted region but upstream of the 6.1 kb P1 promoter. We examined the sequence homology among mouse, rat, human, orangutan, dog, horse, opossum, and chicken in the deleted region, and found that a 1.3 kb region located about 30 kb upstream of the transcription start site of type II *Runx2* was highly conserved among all of the species (Fig. 3A). Using the 1.3 kb fragment and the Hsp68 minimal promoter, we generated GFP tg (1.3kE GFP tg) mice. Gross appearance showed GFP expression in skeletons, and GFP was detected in osteoblasts but not in chondrocytes and non-skeletal tissues on histological analysis (Fig. 3B-I).

A 343 bp enhancer for osteoblast-specific expression and its regulation by Tcf7, Ctnnb1, Smad1, Sp7, and Sox5/6

To find the essential sequence for osteoblast-specific expression in the 1.3 kb enhancer, the 1.3 kb fragment was serially deleted. The deletion to 343 bp maintained the reporter activity of the 1.3 kb fragment with a minimum reduction (data not shown). Further, the sequence of the 343 bp fragment was especially conserved among mouse, rat, human, orangutan, dog, horse, opossum, and chicken in the 1.3 kb fragment. Therefore, we focused on the 343 bp fragment. GFP tg mice driven by the 343 bp fragment and Hsp68 minimal promoter (343E GFP tg mice) showed GFP expression in skeletons, and GFP was detected in osteoblasts but not in chondrocytes and non-skeletal tissues (Fig. 4A-D).

Next, we examined the enhancer activity by reporter assays using the 343 bp fragment (p343-343-luc). Addition of either Wnt3a, BMP2, or TGF-β enhanced the reporter activity, and the combination of Wnt3a and BMP2 and that of Wnt3a and TGF-β synergistically enhanced it (Fig. 4E). We screened the expression cDNA library and found that *Sp7*, *Ctnnb1*, *Smad1*, *Sox5*, and *Sox6* enhanced the reporter activity (Fig. 4F). *Tcf7* and *Smad1* most strongly enhanced the reporter activity among their families, and *Sox5* and *Sox6* were expressed in calvaria and primary osteoblasts (Supplemental Fig. 6A-D). *Smad1*, *Smad2*, *Sp7*, and *Sox5* enhanced the reporter activity synergistically with *Tcf7* and *Ctnnb1* (Fig. 4G). Although the levels of *Runx2* mRNAs were similar in wild-type and $Sp7^{-/-}$ skeletons, expression of other Sp family genes including *Sp1*, *Sp3*, *Sp4*, *Sp5*, and *Sp6*, were upregulated in $Sp7^{-/-}$ skeletons, and *Sp1* and *Sp3* also activated the 343 bp enhancer (Supplemental Fig. 7A-D).

An 89 bp core sequence of the osteoblast-specific enhancer

To find the core sequence in the 343 bp fragment, the former 343 bp fragment in the p343-343-luc vector was serially deleted (Fig. 5A). We found that an 89 bp fragment was sufficient to induce the reporter activity. Further, the combination of Wnt3a and BMP2 and that of Wnt3a and TGF-β synergistically enhanced the reporter activity of p89-89-luc (Supplemental Fig. 7E). In vivo, the 89 bp fragment maintained GFP expression in osteoblasts, although the frequencies of the transgenic mice that expressed GFP in osteoblasts were reduced and the level of the expression was also decreased (Fig. 5B). In GFP tg mice with four tandem repeats of the 89 bp fragment (4x89E GFP tg mice), however, the osteoblasts in all of the tg mice strongly expressed GFP, although GFP was also detected in prehypertrophic and hypertrophic chondrocytes (Fig. 5C-F).

Mef2c and Dlx5 play important roles in the regulation of the 343 bp enhancer

We also searched for the DNA-binding motifs in the 343 bp enhancer sequence. One Mef2-binding motif and one homeobox motif were found in the core 89 bp sequence (Fig. 6A). Among Mef2 family genes, *Mef2c* was relatively highly expressed in skeletal tissues (Supplemental Fig. 6E-H). The introduction of *Mef2c* strongly enhanced the reporter activities of p343-343-luc, p162-343-luc, and p89-343-luc, and the siRNA for *Mef2c* severely reduced the basal activity of p343-343-luc and the activities enhanced by Tcf7/Ctnnb1, Smad1, and Sox6. (Fig. 6B-D).

Next, we examined the effects of *Dlx5* and *Msx2* on the reporter activity of p343-343-luc, because both

homeobox genes are involved in osteoblast differentiation.[16, 17] *Dlx5* alone had no effect on the reporter activity, whereas its combination with *Mef2c* enhanced it. Further, the introduction of *Dlx5* with *Mef2c*, *Tcf7*/Ctnnb1, *Smad1*, and *Sox6* strongly enhanced it (Fig. 6E). In contrast to *Dlx5*, *Msx2* inhibited the basal activity of p343-343-luc and the activities enhanced by Tcf7/Ctnnb1, Mef2c, Smad1, and Sox6 (Fig. 6E). The introduction of *Mef2c*, *Dlx5*, *Tcf7*, *Ctnnb1*, *Smad1*, *Sox6*, and *Sp7* strongly induced the activity of p89-89-luc but the absence of each of them reduced the activity (Fig. 6F). Further, these seven expression vectors induced the reporter activity of p4x89-luc 10 times more than that of p343-343-luc, and they also induced the activity of the reporter vector containing the single 89 bp (p89-luc) in primary osteoblasts (Fig. 6G).

Mutation of the Mef2-binding motif {mut(M)} reduced the reporter activity of p343-343-luc and the enhancement not only by *Mef2c* but also by *Tcf7*/*Ctnnb1*, *Smad1*, *Sox6*, *Sp7*, and *Dlx5* (Fig. 6H-J). Mutation of the homeobox motif {mut(H)} also showed the similar results. Further, the combined mutations of Mef2 and homeobox motifs {mut(M+H)} completely abolished the reporter activities. Further, the mutation of either Mef2 or homeobox motif almost completely abolished the GFP expression in osteoblasts (Fig. 6K-M and data not shown).

Formation of an enhanceosome and histone modifications of the enhancer

In EMSA, Mef2c, Dlx5, and Msx2 but not Tcf7, Ctnnb1, Smad1, Sox6, and Sp7 directly bound to the 89 bp core sequence (Fig. 7A, B, Supplemental Fig. 7F). In GST-pulldown experiments, Dlx5 interacted with Tcf7, Ctnnb1, Mef2c, Sox6, Smad1, and Sp7 (Fig. 7C); Mef2c interacted with Tcf7 and Sox6, and weakly with Sp7

(Fig. 7D); Tcf7 interacted with Ctnnb1, Sox6, Smad1, and Sp7, and Ctnnb1 interacted with Sox6 and weakly with Sp7 (Fig. 7E); and Sox6 interacted with Smad1 and Sp7, and Smad1 interacted with Sp7 (Fig. 7F).

In ChIP analysis, the bindings of Dlx5, Dlx6, Msx2, Mef2, Tcf7, Ctnnb1, Smad1, Sox5, Sox6, and Sp7 to the 343 enhancer region were detected using each antibody, while the binding of Foxa2 was not detected in primary osteoblasts despite the presence of a conserved Foxa2 binding motif in the core 89 bp sequence (Fig. 8A). The bindings of p300 and CBP but not PCAF were detected. In uncommitted mesenchymal cells, C3H10T1/2, the binding of Msx2 but not Dlx5 to the 343 bp enhancer region was detected, whereas the binding of Dlx5 was dominant in osteoblastic MC3T3-E1 cells (Fig. 8B). The enhancer was highly enriched for histone H3 mono- and dimetylated at Lys4 and acetylated at Lys27 and Lys18, but depleted for histone H3 trimethylated at Lys4 in primary osteoblasts. Further, the histone variant H2A.Z was enriched in the enhancer (Fig. 8C). These histone modifications and the enrichment of H2A.Z are the typical features of enhancers.[18] The combination of *Dlx5*, *Mef2c*, *Tcf7*, *Ctnnb1*, *Sp7*, *Sox6*, and *Smad1* enhanced the acetylation of Lys18 and Lys27 in C3H10T1/2 cells, and induced *Runx2* mRNA in C3H10T1/2 cells and primary osteoblasts (Fig. 8D, E).

Discussion

Previous reports showed the importance of the bindings of FosB/JunD, Tcf7/Ctnnb1, Sp1/Elk1, Dlx5, Msx2, and Hoxa10 at various sites in the proximal 700 bp region of *Runx2* P1 promoter for the activation or repression of P1 promoter reporter vectors.[4-8] However, reporter tg mice driven by the 3 kb or 6.1 kb P1

promoter failed to express the reporter genes in osteoblasts (Supplemental Fig. 1).[9] We identified a 1.3 kb osteoblast-specific enhancer about 30 kb upstream of the transcription initiation site of the P1 promoter, which is conserved among many species. The 343 bp fragment, which is especially highly conserved within the 1.3 kb enhancer, was enough for osteoblast-specific expression. Further, the 89 bp core sequence could direct transgene expression to osteoblasts, although the entire 343 bp fragment was required for specific, stable and enhanced expression in osteoblasts.

GFP was not detected in cartilage in GFP tg mice containing the 1.3 kb, 343 bp, and single 89 bp enhancer elements. However, GFP was detected in the growth plates in 4x89E GFP tg mice. Probably, the artificial repeats of 89 bp four times enabled GFP expression in chondrocytes. It may indicate that the 89 bp core sequence contains some elements required for the expression in chondrocytes but they are not sufficient for it. We speculate that other enhancer elements in addition to the 89 bp core sequence are required for Runx2 expression in chondrocytes.

Dlx5 and Mef2c directly bound to the 343 bp enhancer, whereas Tcf7, Smad1, Sox6, and Sp7 did not. Further, mutation of either homeobox motif or Mef2-binding motif abolished the expression in osteoblasts, indicating that Dlx5 and Mef2c play an important role in directing *Runx2* expression to osteoblast lineage cells. From the data of protein-protein interaction and ChIP analyses, a plausible enhanceosome formed by the transcription factors and the cotranscription factor examined in this paper is shown in Fig. 8F. Indeed, p300 and CBP, which bound to the 343 bp enhancer, and other factors including chromatin-remodeling factors should be included in the enhanceosome. The introduction of *Msx2* severely reduced the basal activities of p343-343-luc

and the enhanced activities by *Tcf7*, *Ctnnb1*, *Mef2c*, *Smad1*, and *Sox6*. Further, the binding of Msx2 but not Dlx5 to the 343 bp enhancer was detected in uncommitted mesenchymal cells, C3H10T1/2, whereas the binding of Dlx5 was dominant in osteoblastic MC3T3-E1 cells. These findings suggest that the binding of Msx2 to the homeobox motif in the 89 bp core sequence disturbs the enhanceosome formation.

Our findings unraveled, at least partly, how *Runx2* expression is specifically directed to the osteoblast lineage. As the 343 bp enhancer was enough to induce osteoblast-specific expression, the enhancer contains sufficient elements to direct *Runx2* expression to osteoblasts. Therefore, the enhancer is useful for screening of drugs for osteoporosis and bone regeneration by targeting *Runx2*, and is also useful as a vector for gene therapy of bone diseases.

Disclosures

All the authors state that they have no conflicts of interest.

Acknowledgments

We thank A. Matsuda and S. Muramatsu for the expression cDNA library, T. Sugahara for the screening of cDNA library, M. Osato for *Hsp68* minimal promoter EGFP expression vector, N. Kanatani, Y. Date, Q. Zhang, Q. Xin for technical assistance. This work was supported by grants from the Japanese Ministry of Education, Culture, Sports, Science and Technology, Japan.

References

1. Komori T. Runx2, a multifunctional transcription factor in skeletal development. J Cell Biochem. 2002;87(1):1-8.

2. Fujiwara M, Tagashira S, Harada H, Ogawa S, Katsumata T, Nakatsuka M, et al. Isolation and characterization of the distal promoter region of mouse Cbfa1. Biochim Biophys Acta. 1999 Sep 3;1446(3):265-72.

3. Park MH, Shin HI, Choi JY, Nam SH, Kim YJ, Kim HJ, et al. Differential expression patterns of Runx2 isoforms in cranial suture morphogenesis. J Bone Miner Res. 2001 May;16(5):885-92.

4. Zambotti A, Makhluf H, Shen J, Ducy P. Characterization of an osteoblast-specific enhancer element in the CBFA1 gene. J Biol Chem. 2002 Nov 1;277(44):41497-506.

5. Lee MH, Kim YJ, Yoon WJ, Kim JI, Kim BG, Hwang YS, et al. Dlx5 specifically regulates Runx2 type II expression by binding to homeodomain-response elements in the Runx2 distal promoter. J Biol Chem. 2005 Oct 21;280(42):35579-87.

6. Hassan MQ, Tare R, Lee SH, Mandeville M, Weiner B, Montecino M, et al. HOXA10 controls osteoblastogenesis by directly activating bone regulatory and phenotypic genes. Mol Cell Biol. 2007 May;27(9):3337-52.

7. Zhang Y, Hassan MQ, Xie RL, Hawse JR, Spelsberg TC, Montecino M, et al. Co-stimulation of the bone-related Runx2 P1 promoter in mesenchymal cells by SP1 and ETS transcription factors at polymorphic purine-rich DNA sequences (Y-repeats). J Biol Chem. 2009 Jan 30;284(5):3125-35.

8. Gaur T, Lengner CJ, Hovhannisyan H, Bhat RA, Bodine PV, Komm BS, et al. Canonical WNT signaling promotes osteogenesis by directly stimulating Runx2 gene expression. J Biol Chem. 2005 Sep 30;280(39):33132-40.

9. Lengner CJ, Drissi H, Choi JY, van Wijnen AJ, Stein JL, Stein GS, et al. Activation of the bone-related Runx2/Cbfa1 promoter in mesenchymal condensations and developing chondrocytes of the axial skeleton. Mech Dev. 2002 Jun;114(1-2):167-70.

10. Maeno T, Moriishi T, Yoshida CA, Komori H, Kanatani N, Izumi S, et al. Early onset of Runx2 expression caused craniosynostosis, ectopic bone formation, and limb defects. Bone. 2011 Oct;49(4):673-82.

11. Ueta C, Iwamoto M, Kanatani N, Yoshida C, Liu Y, Enomoto-Iwamoto M, et al. Skeletal malformations caused by overexpression of Cbfa1 or its dominant negative form in chondrocytes. J Cell Biol. 2001 Apr 2;153(1):87-100.

12. Kamekura S, Kawasaki Y, Hoshi K, Shimoaka T, Chikuda H, Maruyama Z, et al.

Contribution of runt-related transcription factor 2 to the pathogenesis of osteoarthritis in mice after induction of knee joint instability. Arthritis Rheum. 2006 Aug;54(8):2462-70.

13. Yoshida CA, Komori H, Maruyama Z, Miyazaki T, Kawasaki K, Furuichi T, et al. SP7 Inhibits Osteoblast Differentiation at a Late Stage in Mice. PLoS One. 2012;7(3):e32364.

14. Muramatsu S, Wakabayashi M, Ohno T, Amano K, Ooishi R, Sugahara T, et al. Functional gene screening system identified TRPV4 as a regulator of chondrogenic differentiation. J Biol Chem. 2007 Nov 2;282(44):32158-67.

15. Yoshida CA, Yamamoto H, Fujita T, Furuichi T, Ito K, Inoue K, et al. Runx2 and Runx3 are essential for chondrocyte maturation, and Runx2 regulates limb growth through induction of Indian hedgehog. Genes Dev. 2004 Apr 15;18(8):952-63.

16. Satokata I, Ma L, Ohshima H, Bei M, Woo I, Nishizawa K, et al. Msx2 deficiency in mice causes pleiotropic defects in bone growth and ectodermal organ formation. Nat Genet. 2000 Apr;24(4):391-5.

17. Robledo RF, Rajan L, Li X, Lufkin T. The Dlx5 and Dlx6 homeobox genes are essential for craniofacial, axial, and appendicular skeletal development. Genes Dev. 2002 May 1;16(9):1089-101.

18. Ong CT, Corces VG. Enhancers: emerging roles in cell fate specification. EMBO Rep. 2012 May;13(5):423-30.

Figure Legends

Figure 1

Reporter gene expression by BAC-derived fragments of *Runx2* gene locus

(A) The constructs of GFP tg mice using a BAC clone. (B-I) Appearance of 200kR (B, C), Δ1st (D, E), Δ2nd (F, G), and Δ3rd (H, I) GFP tg mice at E16.5. (J-Q) Serial frontal sections crossing eyeballs in Δ1st (J-M) and Δ2nd (N-Q) GFP tg mice at E16.5. The upper side of eyeballs (J, L, N, P) and the lower side of eyeballs (K, M, O, Q) are shown. e, eyeball; f, frontal bone; c, connective tissue; z, zygomatic bone; m, maxilla. The mandibles in 200kR, Δ2nd, and Δ3rd GFP tg mice are strongly GFP-positive (single white arrows in B, F, H), whereas that in Δ1st GFP mouse is GFP-negative (single white arrow in D). Double arrows in B, D, F, and H show the GFP expression in the frontal and basal regions of eyeballs. The shape of the GFP-expressed regions (double arrows) is crescent in 200kR, Δ2nd, and Δ3rd GFP tg mice (B, F, H) but linear in Δ1st GFP tg mouse (D). Histological analysis revealed that the double arrows in B, F, and H indicate GFP expression in the zygomatic bones and maxillas, whereas the double arrows in D indicate GFP expression in the surface of the zygomatic bone (Fig. 1K, M, O, Q). The arrowheads in D indicate GFP expression in connective tissues (Fig. 1J, L). The GFP expression in the frontal bones is evident in 200kR, Δ2nd, and Δ3rd GFP tg mice (B, F, H, N, P) but not in Δ1st GFP tg mice (D, J, L) (asterisks in B, D, F, H), whereas the whole brain region was weakly GFP-positive in Δ1st GFP tg mice but not in the others (red arrows in B, D, F, H), probably reflecting GFP expression in neurons in Δ1st GFP tg mice. The arrowheads in J-Q indicate the connective tissue around choroid. Bar = 2 mm

in (B-I) and 100 μm (J-Q).

Figure 2

Histological analysis of GFP tg mice

Frozen sections of mandibles (A, C, E, G, I) and femurs (B, D, F, H, J) from wild-type (A, B), 200kR GFP (C, D), Δ1st GFP (E, F), Δ2nd GFP (G, H), and Δ3rd GFP (I, J) tg mice at E16.5 are shown. Two lines of each genotype were established and showed a similar expression pattern. The expression levels of the transgene in both of 200kR GFP tg mouse lines were low, while those in one of the two lines in Δ1st, Δ2nd, and Δ3rd GFP tg mice were high and the pictures of the strong lines are shown. The pictures of wild-type and 200kR GFP tg mice were taken with a longer exposure time compared with that used for Δ2nd and Δ3rd GFP tg mice. Although the transgene expression level was high in the Δ1st GFP tg mouse line, the GFP expression in bones was too weak to detect, and the pictures of the bone tissues were taken with a longer exposure time compared with that used for Δ2nd and Δ3rd GFP tg mice. m, Meckel's cartilage. Bar = 100 μm.

Figure 3

1.3 kb osteoblast-specific enhancer

(A) Homology of rat (R), human (Hu), orangutan (Or), dog (D), horse (H), opossum (Op), and chicken (C) sequences against mouse sequence in the upstream region of exon 1 of *Runx2* searched by UCSC Genome Browser. 1.3kE: 1.3 kb enhancer, P1:6.1 kb P1 promoter. (B-I) 1.3kE GFP tg mouse at E16.5. Bright and dark field pictures are merged in C. The numerator in B indicates the number of F_0 transgenic mice with osteoblast-specific expression and the denominator indicates the number of F_0 GFP-expressing tg mice obtained.

(D) mandible, (E) head, (F) femur, (G) heart, (H) liver, (I) spinal cord. m, Meckel's cartilage; b, brain; gp, growth plate; h, heart; lu, lung; li, liver; sc, spinal cord. Bar = 5mm in (B, C) and 100 μm in (D-I).

Figure 4

343 bp osteoblast-specific enhancer

(A-D) Appearance (A) and frozen sections of the head (B), mandible (C), and femur (D) of 343E GFP tg mouse at E16.5. The numbers in A indicate the same as those in Fig. 3B. The growth plate is outlined in D. b, brain; m, Meckel's cartilage; gp, growth plate. Bar = 5mm in (A); 100 μm in (B-D). (E-G) Reporter assays. E, Induction of the reporter activity of p343-343-luc by various ligands. RA, retinoic acid. F, Induction of the reporter activity of p343-343-luc by transcription factors. G, Synergistic effects with *Tcf7*/*Ctnnb1* in the induction of the reporter activity of p343-343-luc.

Figure 5

Deletion of the 343 bp enhancer

(A) Deletion constructs of p343-343-luc and their reporter activities. (B) 89E GFP tg mouse at E16.5. (C-F) Appearance (C) and frozen sections of craniofacial region (D) and lower limb (E) of 4x89E tg mouse at E16.5. Boxed region in E is magnified in F. Asterisk shows prehypertrophic and hypertrophic chondrocytes, and double asterisks show osteoblasts. The numbers of F_0 tg mice with expression in osteoblasts are shown in B and C. f, frontal bone; ma, mandible; fe, femur; t. tibia. Bar = 5mm in (B, C); 1 mm in (D); and 0.5 mm in (E, F).

Figure 6

Activation of 343 bp enhancer by *Mef2c* and *Dlx5*

(A) Homeobox and Mef2-binding motifs in the core 89 bp sequence and generation of their mutations. (B) Reporter assay using the deletion constructs of p343-343-luc in SaOS2 cells. (C) The effect of *Mef2c* siRNA on the mRNA expression of Mef2 family genes using SaOS2 cells. The expression was examined by real-time RT-PCR and the ratios against control siRNA are shown. (D) The effect of *Mef2c* siRNA on the activity of p343-343-luc. (E) The effects of *Dlx5* and *Msx2* on the activity of p343-343-luc using MC3T3-E1 cells. (F) Reporter activity in the presence of *Tcf7*, *Ctnnb1*, *Mef2c*, *Smad1*, *Sox6*, *Dlx5*, and *Sp7*, and those in the absence of each of them on p89-89-luc in C3H10T1/2 cells. (G) Induction of reporter activities of p343-343-luc, p4x89-luc, and p89-luc by *Tcf7*, *Ctnnb1*, *Mef2c*, *Smad1*, *Sox6*, *Dlx5*, and *Sp7* (all) in primary osteoblasts. (H-J) Reporter assay using p343-343-luc with mutation(s) in the Mef2 motif (M), homeobox motif (H), or both (M+H) in SaOS2 cells (H, I) and C3H10T1/2 cells (J). In J, *Tcf7*, *Ctnnb1*, *Mef2c*, *Smad1*, and *Sox6* with or without *Dlx5* were introduced. The ratios of *+Dlx5*/*-Dlx5* are shown. (K-M) The pictures of 343E tg mice with a mutation in Mef2 (K, L) or homeobox motif (M). One out of 17 343E tg mice with a mutation in Mef2 motif showed GFP expression in mandible, zygomatic bone, frontal bone, limb bones, and ribs, which is similar to 343E tg mice (Fig. 4A), although the expression level was weak (K). A representative picture of the other 16 343E tg mice with a mutation in Mef2 motif, all of which showed no GFP expression in bones, is shown in L. GFP was detected in skin in this mouse by histological analysis (data not shown). None of 15 343E tg mice with a mutation in homeobox motif showed GFP expression in bones. A representative picture of the 15 mice is shown in M. The arrow indicates GFP expression in mesenchymal cells around the tooth buds, and the arrowhead indicates GFP expression in neurons in the brain (M), which were confirmed by histological analysis

(data not shown). The number in K indicates the frequency of the mice with GFP expression in bone, and the numbers in L and M indicate the frequencies of the mice without GFP expression in bones. Bar = 5mm.

Figure 7

EMSA and GST-pulldown experiment

(A, B) EMSA using 70 bp oligonucleotides covering homeobox and Mef2 motifs (A), 26 bp oligonucleotides covering Mef2 motif and 27 bp oligonucleotides covering the homeobox motif (B) in the core 89 bp sequence. Arrow indicates the specific band of Mef2c, arrowhead indicates the specific band of Dlx5, and asterisk indicates the specific band of Msx2. (C-F) GST-pulldown experiments. G, GST; F, flag; inp, input.

Figure 8

ChIP and real-time RT-PCR analyses

(A-C) ChIP analysis in the 343 enhancer region using primary osteoblasts (A, C), and C3H10T1/2 cells (left) and MC3T3-E1 cells (right) (B). 2μg of antibodies against H3K4me1, H3K4me3, H3K18ac, H3K27ac, and H2A.Z and 0.2 μg of antibody against H3K4me2 were used for immunoprecipitation in C. (D, E) Acetylation of histone (D, ChIP analysis) and *Runx2* mRNA induction (E, real-time RT-PCR analysis) by the combination of *Dlx5*, *Mef2*, *Tcf7*, *Ctnnb1*, *Sox6*, *Smad1*, and *Sp7* (all) in C3H10T1/2 cells and primary osteoblasts (POB). Immunoprecipitated DNA was quantified by real-time PCR and the ratios against IgG are shown in D. (F) Predicted enhanceosome on the 89 bp core sequence.

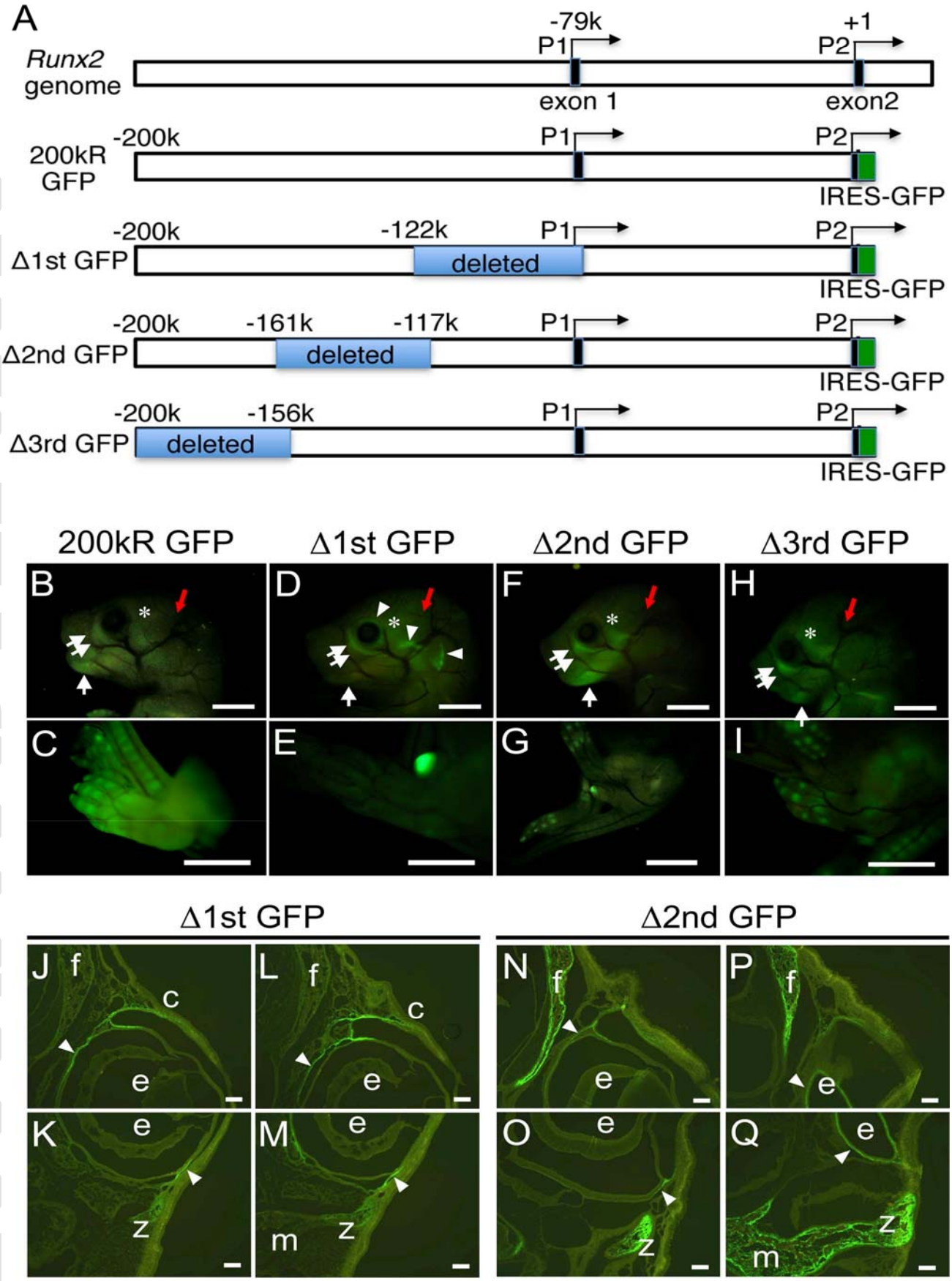

Fig. 1

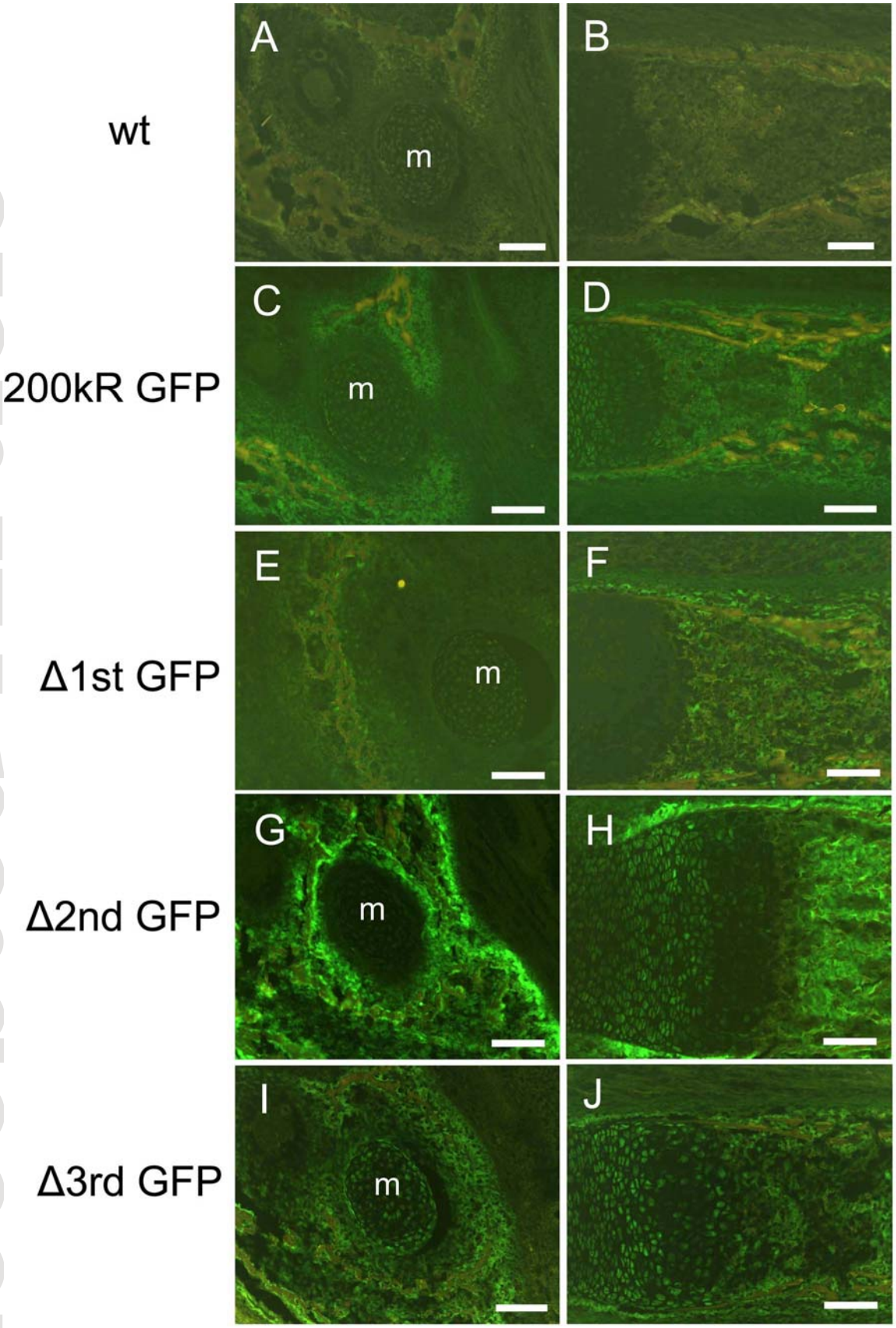

Fig. 2

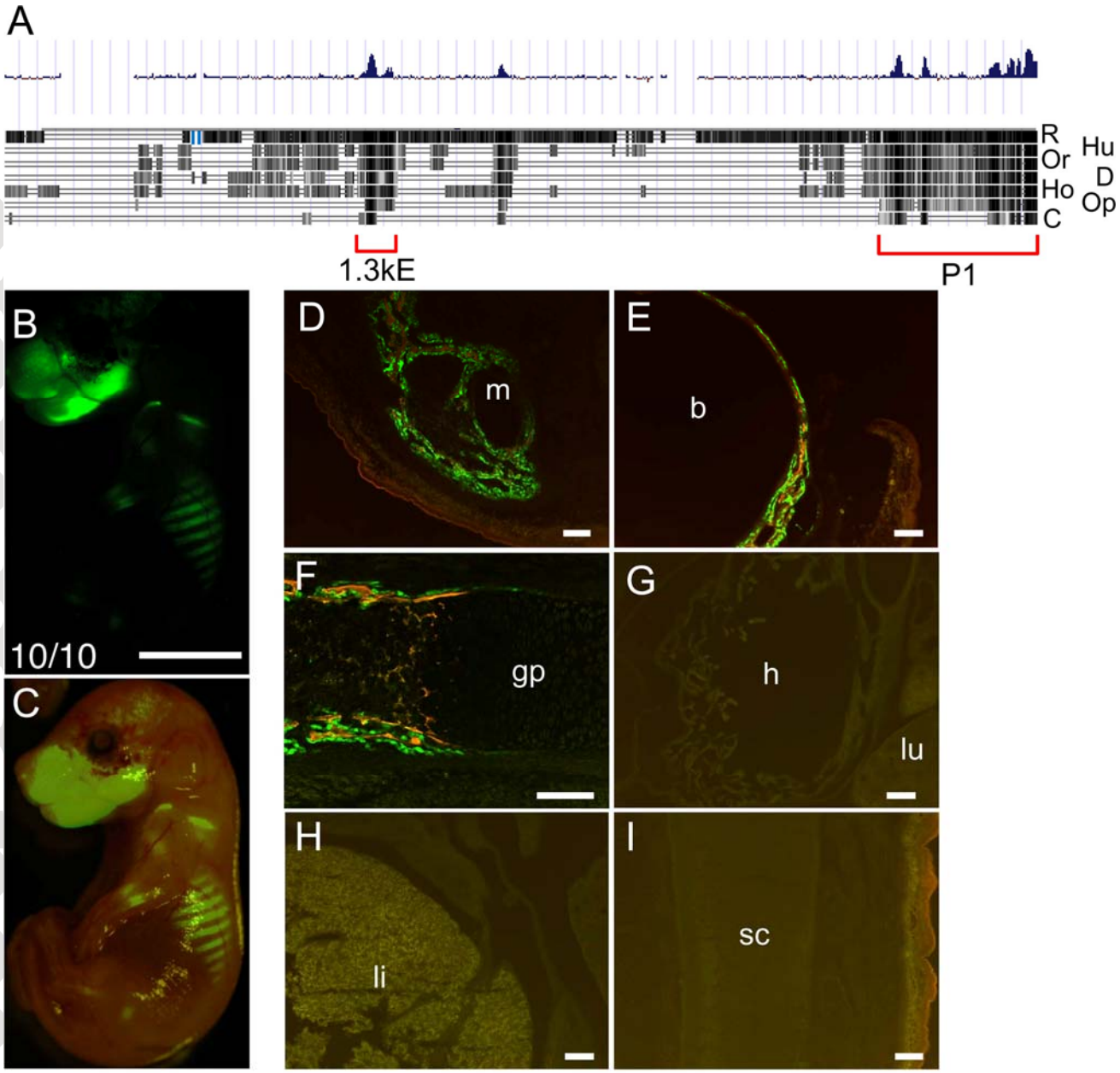

Fig. 3

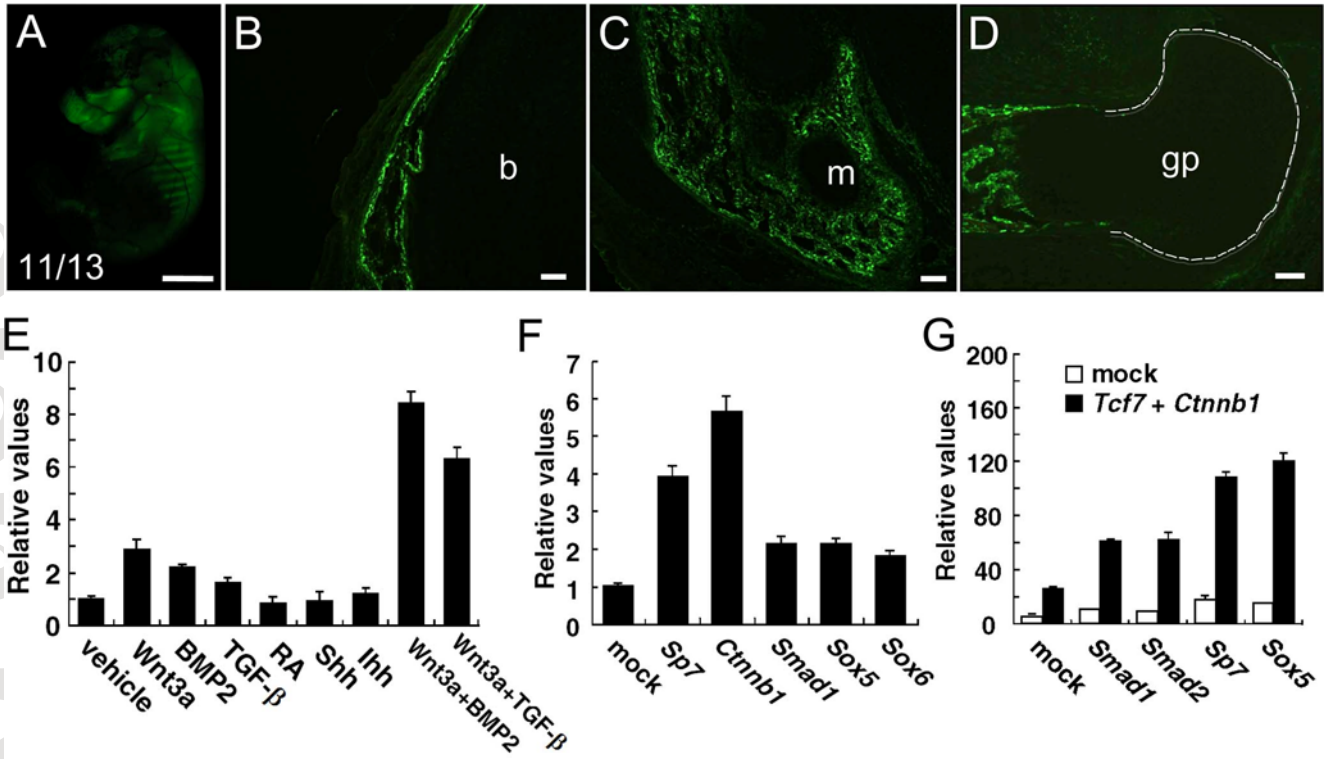

Fig. 4

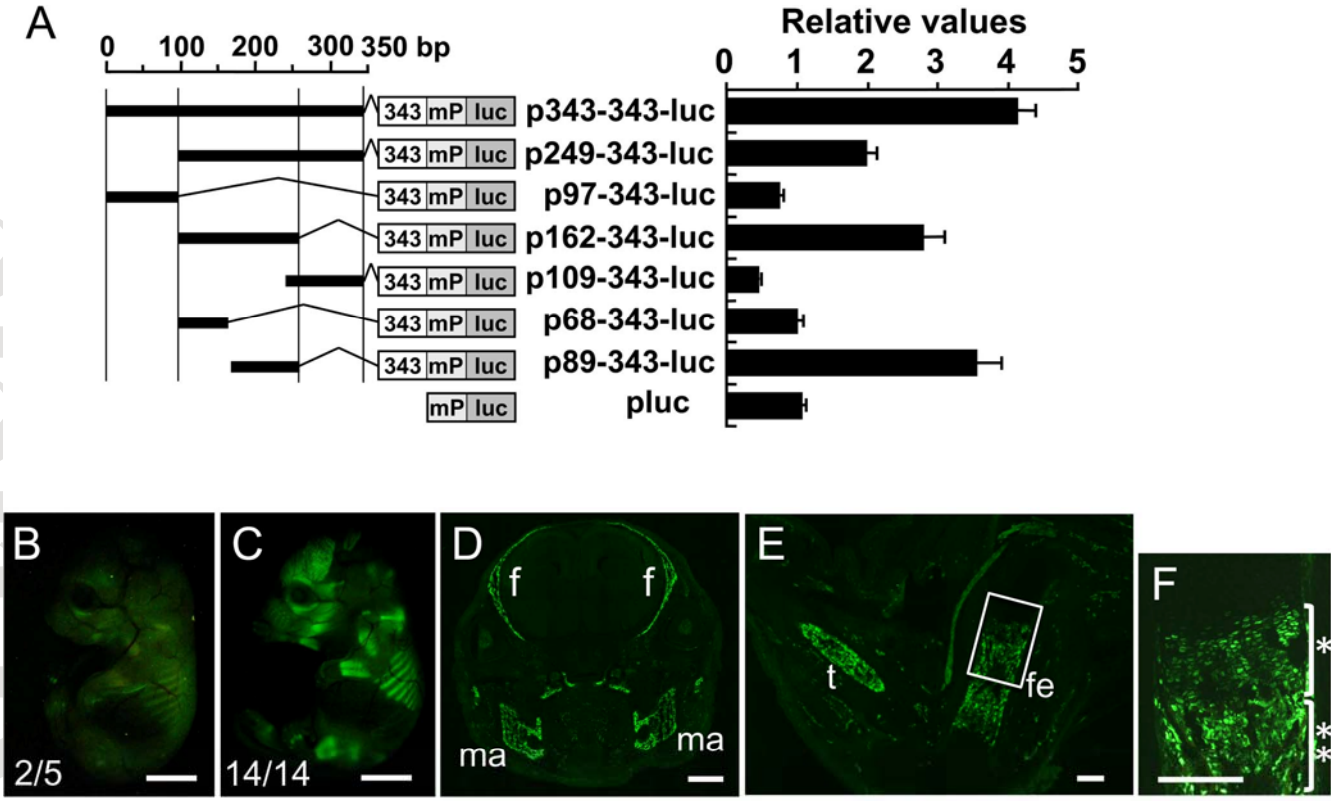

Fig. 5

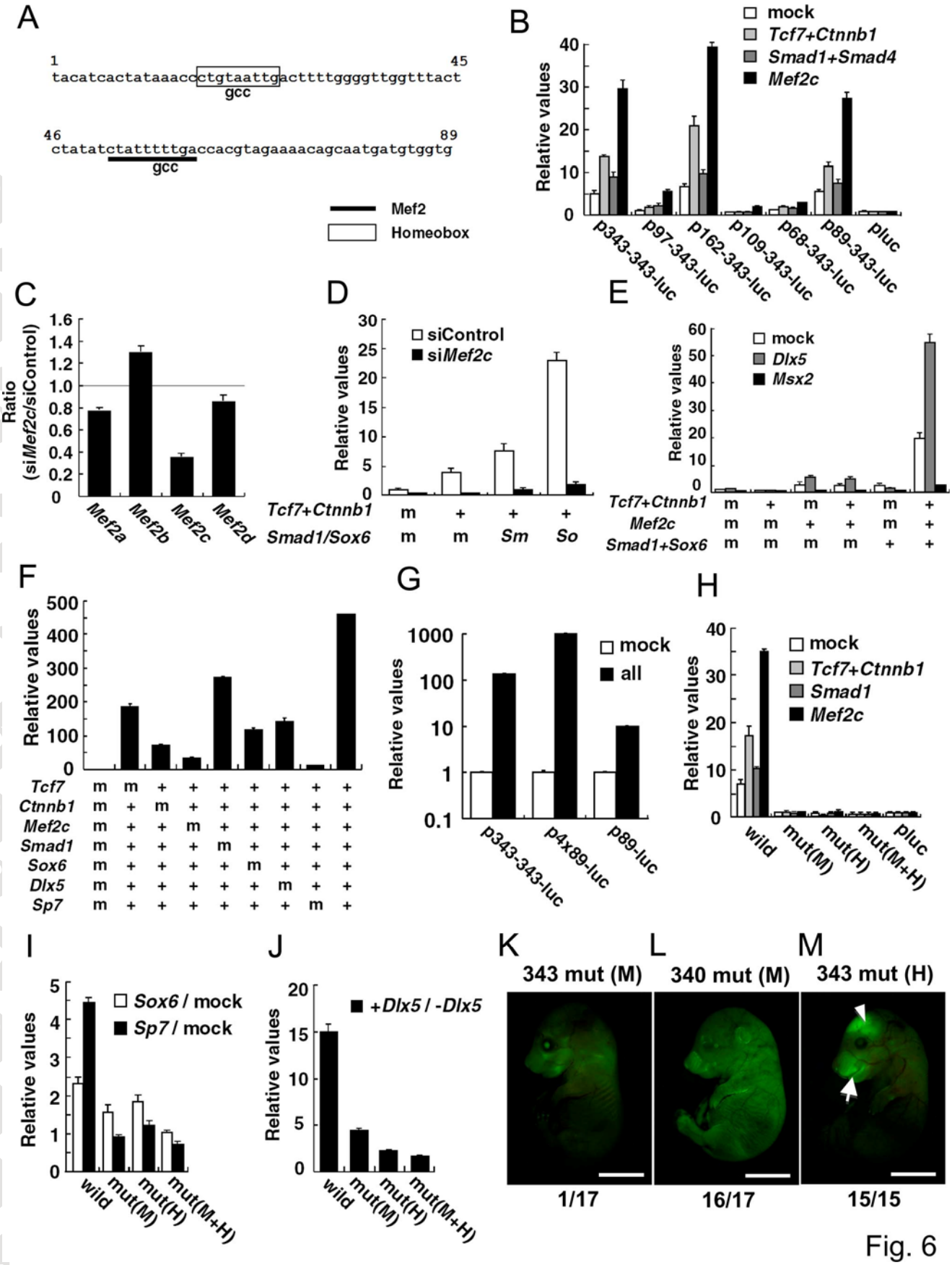

Fig. 6

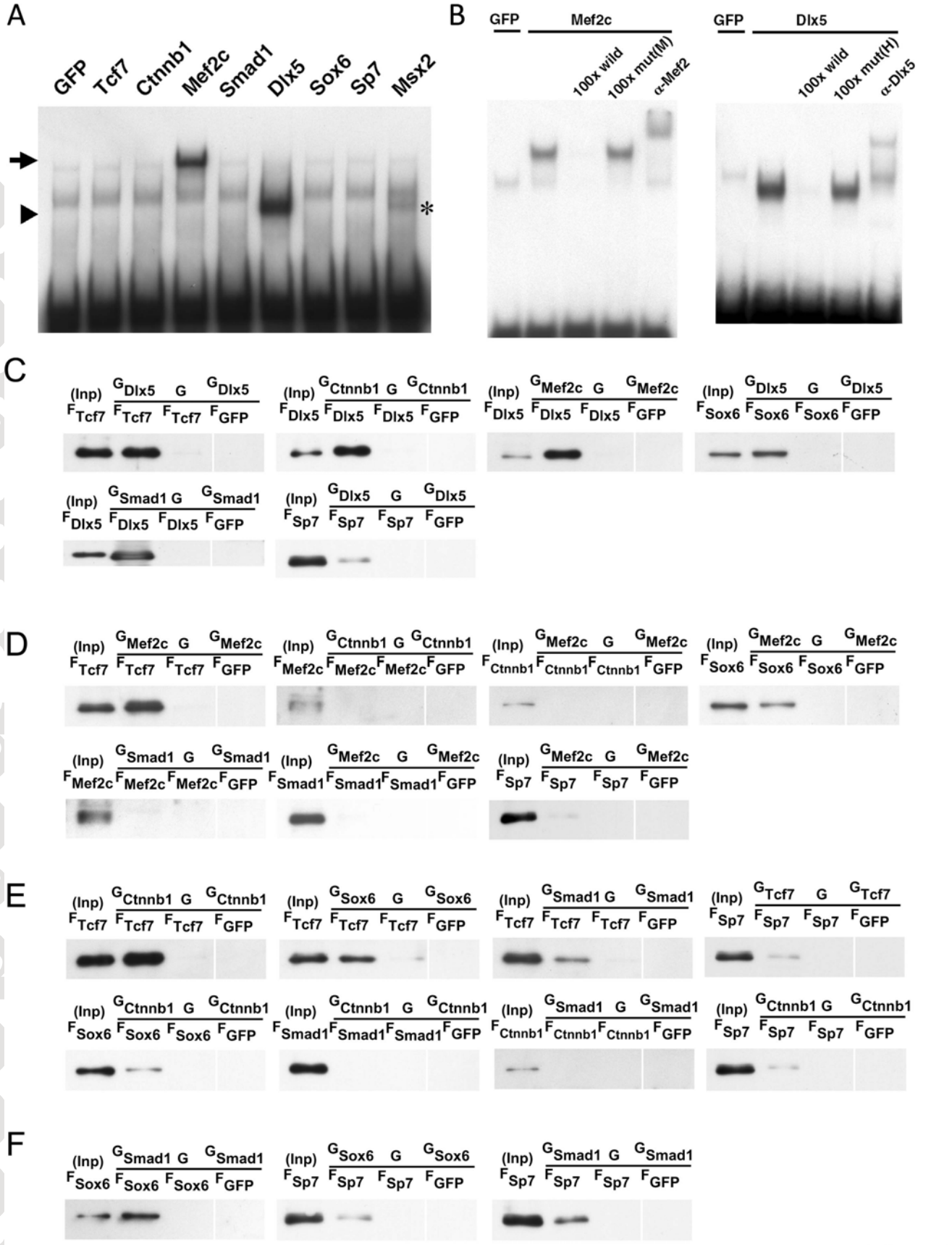

Fig. 7

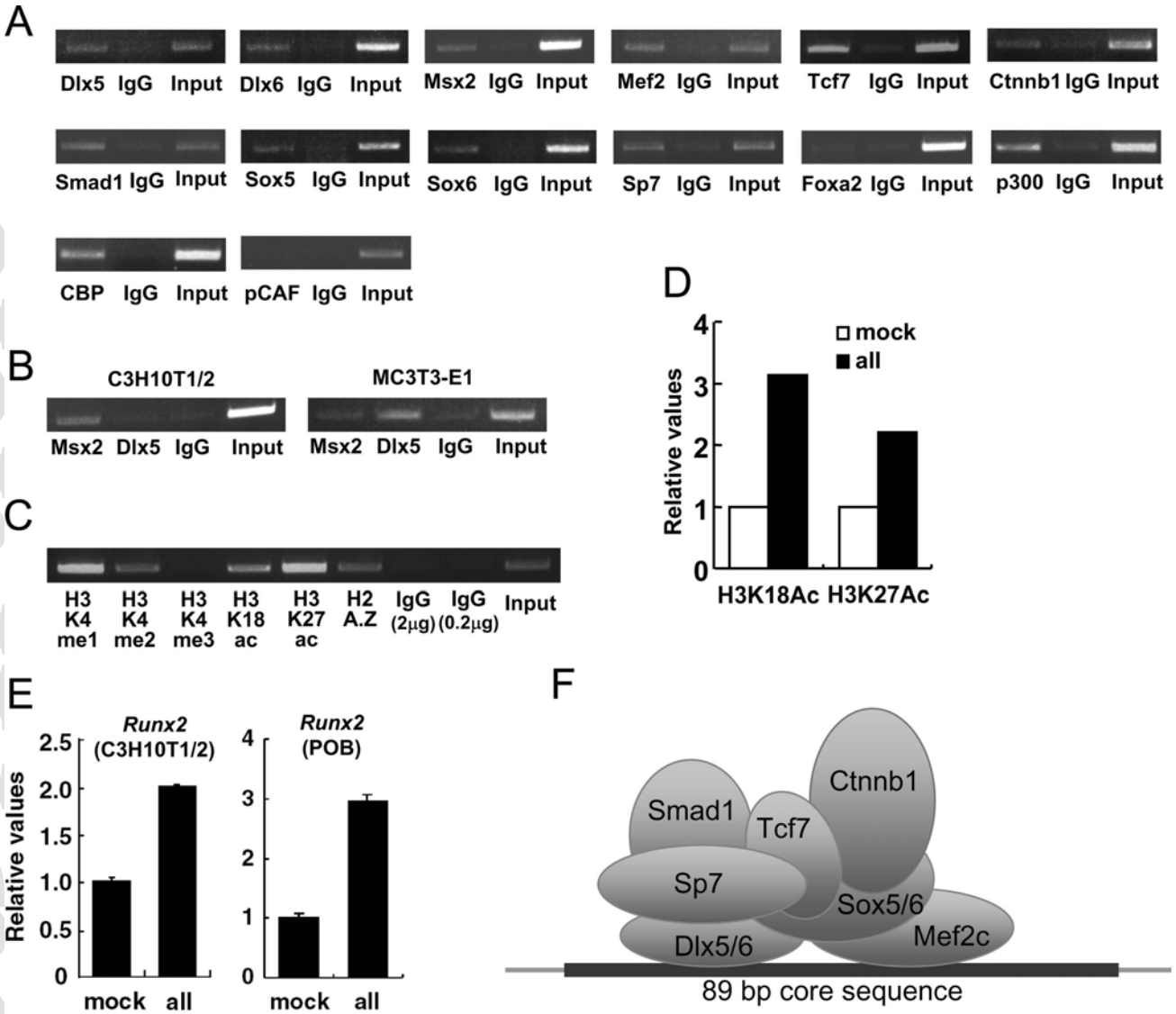

Fig.8